Electromagnetic η_i mode turbulence at the plasma edge

A. Zeiler, K. Hallatschek, D. Biskamp
Max-Planck-Institut für Plasmaphysik, EURATOM Association, 85748 Garching, Germany
J. F. Drake, B. N. Rogers
Institute for Plasma Research, University of Maryland, College Park, MD 20742, USA

Electromagnetic toroidal η_i mode turbulence is investigated linearly and nonlinearly for parameters typical for the plasma edge. The linear eigenmodes are shifted to longer wavelength while the growth rate remains unchanged, thus a mixing length estimate would predict an increase of the transport rates. Nonlinear simulations, however, exhibit a strong drop of the transport rates, when electromagnetic effects are taken into account. This reduction of the transport rates is associated with a fundamental change in the dominant scale lengths and saturation of the underlying turbulence. Specifically, magnetic reconnection plays a dominant role in the nonlinear evolution. Therefore magnetic fluctuations should generally be included in simulations of η_i mode turbulence.

1 Introduction

During the last years large efforts have been taken to achieve a theory based understanding of the anomalous transport in tokamaks. Plasma edge turbulence exerts vital control on the overall confinement by determining the height of the edge pedestal which enters most core confinement scalings as the dominant external parameter. Edge turbulence is typically characterized by three different regimes [1]: At the outermost, low temperature edge resistive ballooning modes provide the dominant drive for the turbulence. In the subsequent region of modestly higher temperature resistivity becomes smaller and the ballooning mode is stabilized by diamagnetic effects. At these parameters the turbulence is maintained by the nonlinear drift wave instability. Raising the temperatures further suppresses the nonlinear drive and destabilizes the toroidal η_i mode at increasingly large scales, in particular when the gradients flatten out towards the top of the edge pedestal. Recently the investigations of the resistive ballooning and the nonlinear drift wave turbulence have been extended to include magnetic fluctuations, and in both regimes major changes compared to the electrostatic limit have been observed for different reasons [2, 3, 4]. Nonlinear simulations of η_i mode turbulence typically still rely on the electrostatic approximation. Thus, it appears to be important to proceed with a complete electromagnetic description, in particular regarding the prominent role of η_i mode turbulence in core confinement physics [5].

2 Equations

Our investigations are based on the drift-Braginskii equations [6] including magnetic pumping but dropping electron thermal effects.

$$(2\pi)^2\alpha_m\left[\partial_t\psi+\alpha_d\partial_y\psi\right]-\nabla_\parallel(\phi-\alpha_d n)=J, \tag{1}$$

$$\nabla_\perp\cdot d_t\nabla_\perp(\phi+\tau\alpha_d p_i)+\hat{C}(p+G)-\nabla_\parallel J=0, \tag{2}$$

$$d_t n+\partial_y\phi-\left[\epsilon_n\hat{C}(\phi-\alpha_d n)-\epsilon_v\nabla_\parallel v_\parallel+\alpha_d\epsilon_n(1+\tau)\nabla_\parallel J\right]=0, \tag{3}$$

$$\begin{aligned} d_t T_i+\eta_i\partial_y\phi-(2/3)\left[\epsilon_n\hat{C}(\phi-\alpha_d n+(5/2)\tau\alpha_d T_i)-\epsilon_v\nabla_\parallel v_\parallel+\alpha_d\epsilon_n(1+\tau)\nabla_\parallel J\right] \\ -(2/3)\kappa_i\nabla_\parallel\left(\nabla_\parallel T_i+(2\pi)^2\alpha_m\eta_i\partial_y\psi\right)=0, \end{aligned} \tag{4}$$

$$d_t v_\parallel=-\epsilon_v\left[\nabla_\parallel(p+4G)+(2\pi)^2\alpha_m[1+\eta_i\tau/(1+\tau)]\partial_y\psi\right], \tag{5}$$

with $J=\nabla_\perp^2\psi$, $p_i=n+T_i$, $p=n+\tau T_i/(1+\tau)$, $G=2\gamma_p\left[\hat{C}(\phi+\tau\alpha_d p_i)-4(\epsilon_v/\epsilon_n)\nabla_\parallel v_\parallel\right]$, and the operators $\nabla_\parallel=\partial_z+(2\pi)^2\alpha_m\vec{z}\times\nabla_\perp\psi\cdot\nabla_\perp$, $d_t=\partial_t+\vec{z}\times\nabla_\perp\phi\cdot\nabla_\perp$, $\nabla_\perp^2=[\partial_x+\Lambda(z)\partial_y]^2+\partial_y^2$, $\hat{C}=[\cos(2\pi z)+\Lambda(z)\sin(2\pi z)-\epsilon]\partial_y+\sin(2\pi z)\partial_x$ with the shear function $\Lambda(z)=2\pi\hat{s}z-\alpha_m[1+\eta_i\tau/(1+\tau)]\sin(2\pi z)$. To facilitate the comparison with previous work [2, 1, 4], we use the normalization for resistive ballooning turbulence $t_0=(RL_n/2)^{1/2}/c_s$, $L_\parallel=2\pi qR$, and $L_\perp=L_\parallel/(1.96\omega_{ce}\tau_e\omega_{ci}t_0)^{1/2}$. This yields the parameters

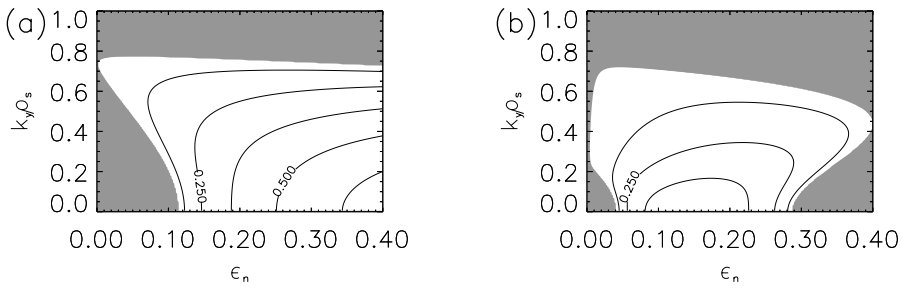

Figure 1: Growth rate $\gamma = -i\omega/\omega_*$ versus ϵ_n and $k_y\rho_s$ for $\tau = 1$, $\eta_i = 2.5$ in the electrostatic limit (a) and for $(2\pi)^2\alpha_m/k_\parallel^2 = 0.3$ (b)

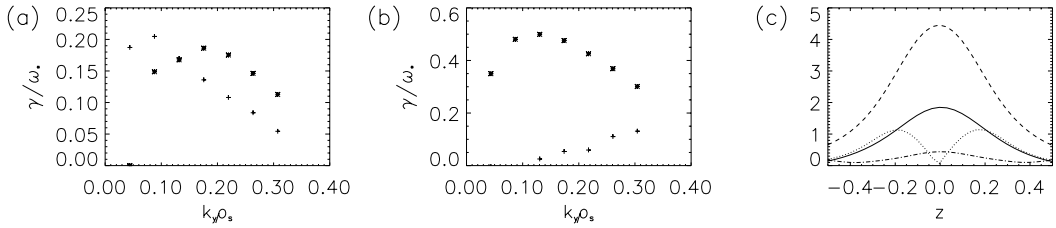

Figure 2: (a) Growth rate versus k_y for the complete set of equations. Parameters are $\eta_i = 2.5$, $\epsilon_n = 0.1$, $\alpha_d = 1.25$, $\kappa_i = 0.005$, $\gamma_p = 0.075$ and $\alpha = 0$ (stars), $\alpha = 0.675$ (crosses). (b) Growth rate with $\epsilon_n = 0.3$, other parameters as in (a). (c) Fluctuation amplitude of n (solid), T_i (dashed), ψ (dotted), and ϕ (dash-dotted) at $\epsilon_n = 0.1$, $k_y\rho_s = 0.18$ versus z (outside of the torus at $z = 0$).

$\alpha_d = v_* t_0/L_\perp$ with v_* the electron diamagnetic velocity, $\epsilon_n = 2L_n/R$, $\epsilon_v = \epsilon_n^{1/2}/(4\pi q)$, and the parallel heat conduction κ_i and the magnetic pumping parameter γ_p. The parameter $\alpha_m = q^2 R\beta/L_n$, finally, is directly related to the usual MHD parameter α by $\alpha_m = \alpha[1 + \eta_i\tau/(1+\tau)]^{-1}$.

3 Linear electromagnetic η_i modes

To qualitatively understand the impact of electromagnetic fluctuations on the linear stability of the toroidal η_i mode we neglect the parallel heat conduction $\kappa_i = 0$, the parallel sound wave $\epsilon_v = 0$, magnetic shear $\hat{s} = 0$ and the resistivity [J term in Eq. (1)], and evaluate the curvature operator $\hat{C}$ at the outside of the torus $z = 0$ (with $\epsilon = 0$). In this limit the only coupling along the magnetic field arises from the shear Alfvén wave, the essential new element compared to the electrostatic regime. With the ansatz $\psi, \phi, n, T_i \propto \exp\{i(k_y y + k_\parallel z - \omega t)\}$ Eqs. (2), (3), and (4) combine to

$$\left[\left(\frac{\omega}{\omega_*}k_y^2\rho_s^2 + \epsilon_n\right)\left(\frac{\omega}{\omega_*} + \frac{5}{3}\tau\epsilon_n + \tau\left(\eta_i - \frac{2}{3}\right)\right) - \left(\frac{\omega}{\omega_*} + \frac{5}{3}\tau\epsilon_n\right)\right]\phi + \tag{6}$$
$$+ \left[\frac{5}{3}\tau\left(\frac{\omega}{\omega_*}k_y^2\rho_s^2 + \epsilon_n\right)\left(\frac{\omega}{\omega_*} + \epsilon_n\tau\right) + \frac{\omega}{\omega_*}\left(\frac{\omega}{\omega_*} + \frac{5}{3}\tau\epsilon_n\right)\right]\alpha_d n = 0,$$

where we have used the abbreviations $\rho_s^2 = \alpha_d^2\epsilon_n(1+\tau)$ and $\omega_* = \alpha_d k_y$. From Eqs. (1) and (3) we obtain a second relation between n and ϕ

$$\left[1 - \frac{(2\pi)^2\alpha_m}{\epsilon_n(1+\tau)k_\parallel^2}\left(\frac{\omega}{\omega_*} - 1\right)(1-\epsilon_n)\right]\phi = \left[1 - \frac{(2\pi)^2\alpha_m}{\epsilon_n(1+\tau)k_\parallel^2}\left(\frac{\omega}{\omega_*} - 1\right)\left(\frac{\omega}{\omega_*} - \epsilon_n\right)\right]\alpha_d n. \tag{7}$$

Eq. (7) is the electromagnetic generalization of the usual adiabatic relation $\phi = \alpha_d n$ which is readily obtained in the electrostatic limit $\alpha = \alpha_m = 0$. With $\phi = \alpha_d n$ Eq. (6) reproduces the dispersion relation of the electrostatic toroidal η_i mode (compare Ref. [1] and citations therein). In Figure 1 we show the result of a numerical evaluation of the dispersion relation obtained from Eqs. (6) and (7). Consistent with earlier results [7] electromagnetic effects stabilize the mode over most of the parameter regime, in particular at large $\epsilon_n \gtrsim 0.3$. At intermediate ϵ_n ($\sim 0.05 - 0.3$), which is typical for the plasma edge near the top of the pedestal, however, long wavelength modes are destabilized. This suggests an increase of the transport rates in this region when electromagnetic effects are taken into account. At small $\epsilon_n \lesssim 0.05$, typical of the outermost edge, the η_i mode remains weak even when α is finite.

ϵ_n	α	$\langle nv_r \rangle$	$\langle T_i v_r \rangle$
0.07	0	0.06	0.53
0.07	0.225	0.053	0.33
0.07	0.675	0.034	0.20
0.1	0	0.083	0.87
0.1	0.675	0.039	0.21

Table 1: $E \times B$ transport rates for different values of ϵ_n and α, $\alpha_d = 1.25$, $\eta_i = 2.5$. For $\epsilon_n = 0.07$ $\kappa_i = 0.0035$, $\gamma_p = 0.05$, and for $\epsilon_n = 0.1$ $\kappa_i = 0.005$, $\gamma_p = 0.075$.

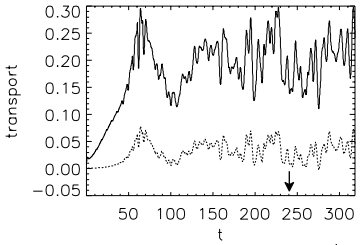

Figure 3: $E \times B$ heat flux $\langle T_i v_r \rangle$ (solid line) and particle flux $\langle nv_r \rangle$ (dotted line) versus time for the parameters $\epsilon_n = 0.07$, $\alpha = 0.675$ and $\eta_i = 2.5$.

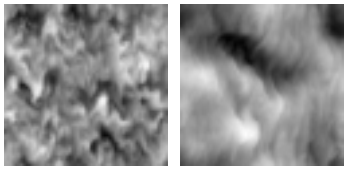

Figure 4: Structure of T_i in the direction perpendicular to the magnetic field at the out side of the torus ($z = 0$). The left plot corresponds to $\alpha = 0$, the right plot to $\alpha = 0.675$.

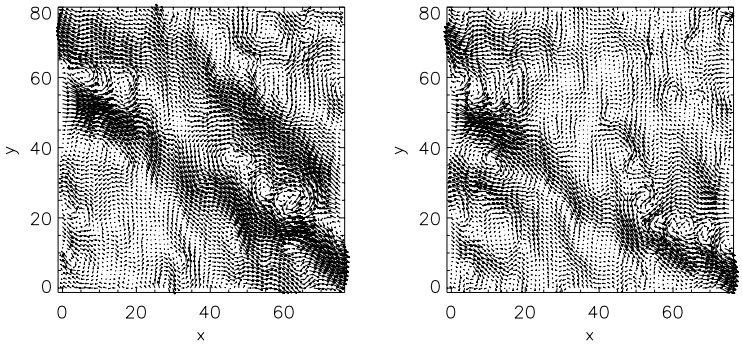

Figure 5: Magnetic reconnection at a late state of the simulation discussed in Fig. 3 (marked by a little arrow in Fig. 3). The left plot shows the magnetic field at $z = -0.83$ (outside of the torus at $z = -1, 0, 1$) and $t = 234$, the right plot at $t = 247$.

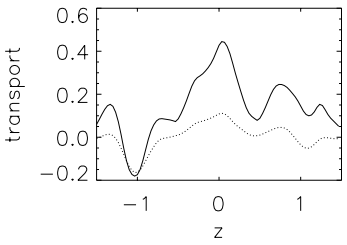

Figure 6: Ion heat flux (solid) and particle flux (dotted) at $t = 244.5$ in the simulation discussed in Figs. 3 and 5.

The importance of electromagnetic effects is controlled by both α and $k_\parallel$ [compare Eq. (7)]. If $k_\parallel$ is sufficiently large, the Alfvén wave is fast enough to establish the adiabatic relation $\phi = \alpha_d n$, even if α is large, and we obtain the electrostatic dispersion relation. In the complete set of equations Eqs. (1) - (5) the parallel gradients are limited by ion heat conduction and the parallel sound wave. To realistically include these effects we evaluate the growth rates with our three-dimensional initial value code [1], where we choose all parameters including the numerical viscosities as in the nonlinear simulations which will be discussed in the next section. Figure 2a confirms our basic result that for typical plasma edge gradients $\epsilon_n \simeq 0.1$ electromagnetic effects destabilize the η_i mode at long perpendicular wavelength, whereas at larger ϵ_n electromagnetic effects strongly reduce the growth rate (Fig. 2b).

4 Nonlinear simulations

Based on our linear results the usual mixing length estimate for the anomalous diffusion coefficients $D = \gamma / k_\perp^2$ predicts a strong increase of the transport for $\epsilon_n \sim 0.1$, as the parameter α is increased. To test this we performed a series of nonlinear simulations with our 3-d flux-tube code [1]. The box dimensions are $80 L_\perp \times 80 L_\perp \times 3 L_\parallel$ at a resolution of $192 \times 192 \times 90$ collocation points. Surprisingly the turbulent transport rates strongly contradict the mixing length estimate (Table 1): raising α from zero to 0.675 leads to a drop of the anomalous heat flux of roughly a factor of three. In the electromagnetic regime the fluxes exhibit large fluctuations, and may even become negative (Fig. 3). The structure of the turbulence in the electromagnetic regime also differs substantially from the electrostatic limit (Fig. 4): whereas in the electrostatic limit the scale size of the fluctuations is several times the ion gyro radius, it becomes very large in the electromagnetic regime. The electromagnetic state is characterized by highly localized eddies in the magnetic field as well as in the $E \times B$ velocity, which have no counterpart in the electrostatic simulations. Within these eddies the plasma velocity considerably exceeds average levels. These strong flows cause the large fluctuations in the fluxes, and can even result in negative values of transport in spatially localized areas.

The failure of the linear mixing length estimate demonstrates that the magnetic fluctuations must also strongly influence the nonlinear saturation of the fluctuations. The fundamental change of the nonlinear dynamics is underscored by the presence of the fast rotating eddies and the large localized fluxes in the direction opposite to the equilibrium gradients. A more detailed analysis of the time evolution shows

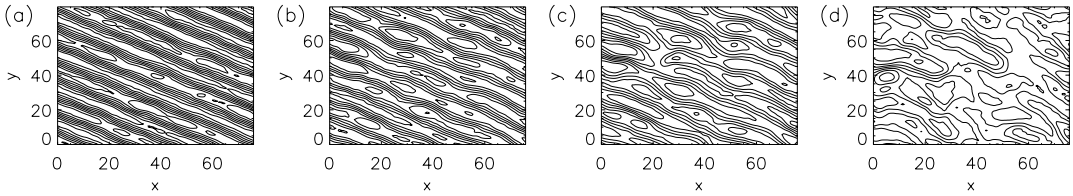

Figure 7: Saturation of the linear mode displayed in Figure 2b. The plots show contours of the magnetic potential ψ at $z = 0.17$ with time increasing from left to right.

that these originate from regions where major changes in the three dimensional topology of the magnetic field occur. Figure 5 shows such an event. Initially the magnetic field consists of two oppositely directed bands of magnetic flux which are separated by a chain of islands (left plot). About ten time units later the sheared structure is completely destroyed (right plot). Finally, Figure 6 shows the transport rate as a function of the parallel coordinate z; we observe strong negative transport at the location where the magnetic field is changed. Thus, magnetic reconnection seems to be responsible for the sharp drops in the transport rates and therefore plays a dominant role in the overall dynamics. To gain some better insight into the saturation mechanisms we use the eigenmode shown in Figure 2c as initial condition in our three-dimensional code and study the nonlinear breakup. The streamers resulting from the toroidal η_i mode (Fig. 7a) are perturbed by an instability with $k_\perp \rho_s \simeq 0.15$ (Fig. 7b). At sufficiently large amplitude of the perturbation the magnetic field starts to reconnect (Fig. 7c), which finally completely destroys the radial streamers (Fig. 7d). It is important to note that the secondary instability starts to grow in the vicinity of the maximum of ψ at $z \simeq 0.2$, not at $z = 0$ where ϕ, n and T_i are peaked (compare Fig. 2c). This indicates that the magnetic energy provides the dominant drive, and therefore suggests that the secondary instability is a tearing mode. To confirm this we performed two-dimensional analytical and numerical calculations on the stability of a sheared magnetic field as in Fig. 7a. The maximum growth rate of the tearing mode is found at $k_x \rho_s \simeq 0.1$ consistent with Fig. 7.

In the electrostatic regime, by contrast, the saturation results from Kelvin-Helmholtz and drift-wave type secondary instabilities as demonstrated for the resistive ballooning mode [2]. Thus, the electrostatic and the electromagnetic regime are characterized by distinct saturation mechanisms, which explains the observed failure of the mixing length approach in comparing the nonlinear transport rates in the electrostatic and the electromagnetic regimes.

5 Summary

Electromagnetic effects alter the growth rate of the toroidal η_i modes in two different ways, depending on the steepness of the profile. For comparatively modest gradients the mode is strongly stabilized. If the gradients are steeper ($L_n \sim 0.5R$), as is typical for the plasma edge near the top of the pedestal, the mode spectrum is shifted to longer wavelength while the peak growth rate is relatively constant. In contrast to a linear mixing length estimate, which would predict an increase of the transport rates in this regime, nonlinear electromagnetic simulations exhibit a strong reduction of particle and heat flux. This reduction is caused by a fundamental change in the nonlinear dynamics: whereas in the electrostatic case the toroidal η_i mode saturates due to the growth of Kelvin-Helmholtz or drift-wave-like secondary instabilities, magnetic reconnection becomes the dominant mechanism in the electromagnetic system. Therefore, certainly in the plasma edge and also possibly in the higher temperature regime of the plasma core, it is essential to keep electromagnetic corrections in simulations of η_i mode turbulence.

References

[1] A. Zeiler, D. Biskamp, J. F. Drake, and B. N. Rogers, Phys. Plasmas **5**, 2654 (1998).
[2] B. N. Rogers, and J. F. Drake, Phys. Rev. Lett. **79**, 229 (1997).
[3] B. Scott, Plasma Phys. Control. Fusion **39**, 1635 (1997).
[4] B. N. Rogers, J. F. Drake, and A. Zeiler, Phys. Rev. Lett. **81**, 4396 (1998).
[5] P. B. Snyder, G. W. Hammett, and M. A. Beer, Bull. Amer. Phys. Soc. **42**, 1986 (1997).
[6] A. Zeiler, J. F. Drake, and B. Rogers, Phys. Plasmas **4**, 2134 (1997).
[7] J. Y. Kim, W. Horton, and J. Q. Dong, Phys. Fluids B **5**, 4030 (1993).